Lattice instability and soft phonons in single-crystal $La_{2-x}Sr_xCuO_4$

P. Böni,* J. D. Axe, and G. Shirane
Brookhaven National Laboratory, Upton, New York 11973

R. J. Birgeneau, D. R. Gabbe, H. P. Jenssen, M. A. Kastner, C. J. Peters,
P. J. Picone, and T. R. Thurston
Center for Materials Science and Engineering, Massachusetts Institute of Technology, Cambridge, Massachusetts 02139

(Received 4 March 1988)

The dispersion of the low-lying phonon branches of several doped and undoped single crystals of $La_{2-x}Sr_xCuO_4$ has been investigated by using inelastic-neutron-scattering techniques. The zone-center modes are in reasonable agreement with Raman measurements. The reported peaks in the phonon density of states show up at energies that correspond to extrema in the dispersion curves of the transverse and longitudinal acoustic branches near the zone boundary. The tetragonal-to-orthorhombic phase transition is caused by a softening of a transverse-optic-phonon mode at the X point. The rotational nature of the soft mode leads to moderate electron-phonon coupling and the mode is unlikely to enhance significantly conventional phonon mediated superconductivity. We did not observe any evidence for the predicted breathing-mode instability near the zone boundary.

I. INTRODUCTION

The cause of the high superconducting temperatures T_c of doped La_2CuO_4 (Ref. 1) and $YBa_2Cu_3O_{7-\delta}$ (Ref. 2) compounds is still an open question, although many experiments and theories have been devoted to this subject in the past year. Several different mechanisms have been suggested to explain the very high critical temperatures of these oxide superconductors, for example, strong[3-6] or weak[7] electron-phonon coupling, resonating valence bonds,[8] anharmonicity,[9] and spin fluctuations.[10,11] Neutron scattering is one of the most powerful experimental tools for investigating the mechanism leading to high T_c because neutrons couple to both phonons and magnetic spin fluctuations and may therefore help in understanding the microscopic processes behind high T_c. This work has been undertaken to investigate the lattice dynamical aspects of this topic.

Let us first review some of the experimental results which are important to the present work.[12] La_2CuO_4 exhibits a tetragonal ($I4/mmm$)-to-orthorhombic ($Cmca$) displacive structural phase transition near $T_0=530$ K caused by a staggered tilting of the oxygen octahedra around the Cu atoms.[13] The dopants Ba or Sr stabilize the tetragonal structure at lower temperature, introduce holes into an otherwise half-filled CuO conduction band, and lead to superconductivity.[14] The recent observation of filamentary superconductivity in undoped La_2CuO_{4-y} (Ref. 15) indicates that the concentration of oxygen is also a very important parameter with regard to the superconducting properties.

Because of the difficulty of growing single crystals of doped La_2CuO_4, most of the phonon data up to now have been obtained from powders or from isostructural compounds. Neutron measurements of the phonon density of states by Renker *et al.*[16] in $La_{2-x}Sr_xCuO_4$ indicate an increased coupling between electrons and high-frequency oxygen vibrations for the superconducting sample but the coupling seems not to be sufficient to explain the high-T_c values. In the low-frequency range, the spectra are almost independent of doping. Hence, it was concluded[16] that soft phonons are not essential for high T_c.

In contrast to these results, Pintschovius *et al.*[17] have found pronounced phonon anomalies in their neutron scattering measurements in La_2NiO_4 (isostructural to La_2CuO_4), which they attribute to a strong renormalization of breathing-type modes.[4] Raman measurements on crystals of $La_{2-x}Sr_xCuO_4$ are mutually inconsistent[18-20] and different conclusions have been drawn. Some measurements support the predicted strong electron-phonon coupling due to breathing-type modes[18] whereas other measurements indicate a lack of a strong coupling.[19] In this regard, it is important to remember that Raman scattering from opaque crystals is only sensitive to the surface, while neutron scattering is a bulk-sensitive method. Recent measurements on samples with different amounts of the isotope ^{18}O in $La_{2-x}Ba_xCuO_4$ (Refs. 21 and 22) and $YBa_2Cu_3O_{7-\delta}$ (Ref. 23) reveal a slight dependence of T_c on the mass of the oxygen atoms and may indicate that phonons play some role in the pairing mechanism for superconductivity. A completely different approach for the explanation of the very high T_c values is based on spin fluctuations. The discovery of antiferromagnetism in La_2CuO_4 (Ref. 24) and very recently $YBa_2Cu_3O_{7-\delta}$ (Ref. 25) and the observation of a very large energy scale for the spin dynamics in the quantum-spin fluid state of La_2CuO_4 (Ref. 26) have given some credence to this alternative approach. Since we will mainly be concerned in this work with the lattice dynamics of the oxide superconductors, we do not go into more details.

We present below neutron measurements of low-energy phonons in single crystals of $La_{2-x}Sr_xCuO_4$. A short ac-

TABLE I. Crystal parameters (Ref. 30) in *Cmca* notation.

Sample	Label	a (Å)	b (Å)	c (Å)	T_0 (K)
$La_{1.97}Sr_{0.03}Cu_{0.95}Li_{0.05}O_{4-\delta}$	MIT-1	5.323	13.084	5.379	351 ± 1
$La_2Cu_{0.95}Li_{0.05}O_{4-\delta}$	MIT-2	5.333	13.098	5.384	423 ± 1
La_2CuO_4	NTT-2	5.339	13.100	5.422	503
La_2CuO_4	NTT-3	5.333	13.095	5.419	499

count of some results has already been given elsewhere.[27] We started these experiments in an attempt to verify the predicted breathing-mode instability. Instead, we observed a more conventional soft-phonon driven tetragonal to orthorhombic phase transition. The observations are in good qualitative agreement with nonempirical calculations by Cohen, Pickett, Krakauer, and Boyer[28] which are based on an ionic model. We present rather complete results for the acoustic phonon branches and discuss some anomalies observed at intermediate momentum transfer $\mathbf{q}$ in the LA phonon branch. In addition, we discuss the critical behavior of the nuclear scattering near T_0.

II. EXPERIMENT

The experiments were conducted on several triple-axis spectrometers at Brookhaven's High-Flux Beam Reactor. Pyrolytic graphite crystals were used as monochromator and analyzer with fixed final energies 5 meV $\leq E_f \leq$ 30.5 meV and different combinations of 20′ and 40′ collimating elements depending on the conflicting requirements of reasonable intensity and resolution. Higher-order neutrons were removed by pyrolytic graphite or cooled Be filters, respectively. For the low-temperature measurements, the samples were mounted on the cold finger of a nitrogen-flow Dewar and for the measurements up to $T=600$ K ($p=1$ bar) inside an air furnace.

The two single crystals $La_{2-x}Sr_xCu_{0.95}Li_{0.05}O_{4-\delta}$ investigated were grown from a flux containing 50 mol% of $Li_4B_2O_5$ and $Sr_yLa_2CuO_4$ with y in the range of 0 to 2.[29] The sample designated by MIT-1 was doped with Sr ($x=0.03$), sample MIT-2 contained no Sr (see Table I). These samples ($V \simeq 200$ mm^3) were neither superconducting nor metallic, one reason being that only about 10% of Sr present in the melt is actually incorporated into the single crystals. Moreover, superconductivity is also suppressed by the incorporation of small amounts of Li at Cu sites.[29] All samples show variable-range hopping behavior $\ln\rho \sim T^{-1/4}$ indicating that the electronic states at the Fermi surface are localized.[27,29] Measurements of typical phonon spectra in pure samples $La_{2-x}Sr_xCuO_4$, which were grown from a CuO flux by Nippon Telephone and Telegraph[30] (samples NTT-2 and NTT-3), confirm that the lattice dynamics are not visibly affected by small amounts of Li, which is expected to replace Cu. In the following, we will use the notation $La_{2-x}Sr_xCuO_4$ for our samples and define momentum transfer in tetragonal units throughout the paper. The results of the two MIT samples are quite similar, with the exception of the temperature for the displacive structural phase transition T_0, which decreases with increasing Sr and Li content as expected.[31] For most of the experiments, we mounted the samples in the (hhl) scattering plane.

III. STRUCTURAL PHASE TRANSITION

The tetragonal-to-orthorhombic phase transition in La_2CuO_4 has already been discussed several years ago by Von Grande, Müller-Buschbaum, and Schweizer[13] and it was recognized that a soft-phonon mode might be implicated. In a first step, we confirmed that our crystals reveal only those reflections (on a relative intensity level of 10^{-5}) which are allowed for the orthorhombic space group *Cmca* (No. 64). Then we measured the temperature dependence of some strong superlattice peaks like $(\frac{1}{2}\,\frac{1}{2}\,2)$ or $(\frac{3}{2}\,\frac{3}{2}\,2)$ in order to determine T_0. Figure 1 demonstrates that the superlattice peak intensities of both samples can well be described by a power law $(T_0-T)^{2\beta}$ with $\beta=0.28$ (see Table II) but different T_0, depending on the dopant concentration. These results indicate that the transition is of second order.

As discussed in Ref. 27, the atomic displacements involved in the transformation are described by a doubly degenerate ($n=2$) order parameter $\{Q_x\}=(Q_a,Q_\beta)$ with X-

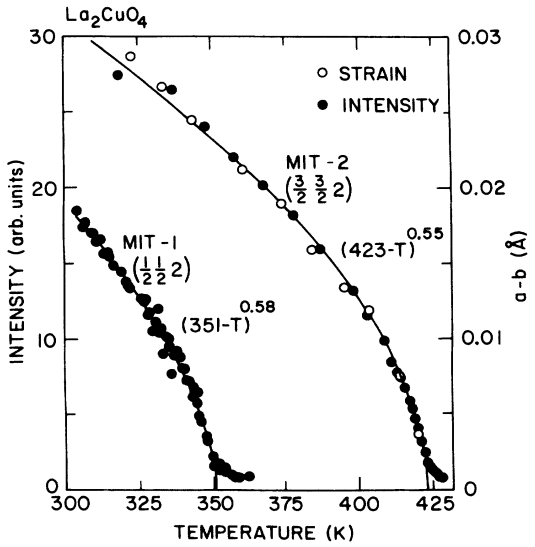

FIG. 1. Superlattice peak intensities in $La_{2-x}Sr_xCuO_4$. The solid lines are fits to the power laws indicated in the figure (see also Table II). Note the excellent scaling between orthorhombic distortion and Bragg intensity for sample MIT-2.

TABLE II. Critical behavior of order parameter, correlation length, susceptibility, and intensity of central peak.

Item	Exponent	Remarks
I_B	$\beta=0.29\pm0.04$	Sample MIT-1
	$\beta=0.275\pm0.04$	Sample MIT-2[a]
I_L	$\gamma=1.23\pm0.05$	
κ	$\nu=0.53\pm0.06$	
I_G	$p=1.04\pm0.13$	

[a]Reference 27.

point wave vectors $\{\mathbf{q}_X\}=(\mathbf{q}_\alpha,\mathbf{q}_\beta)$, where $\mathbf{q}_\alpha=(\frac{1}{2},\frac{1}{2},0)$ and $\mathbf{q}_\beta=(\frac{1}{2},-\frac{1}{2},0)$. The primitive lattice vectors can be written as $\mathbf{b}_1=(0,1,1)$, $\mathbf{b}_2=(1,-1,0)$ and $\mathbf{b}_3=(1,0,-1)$ in terms of the conventional tetragonal lattice vectors and, thus, $-\mathbf{q}_\alpha=\mathbf{q}_\alpha-\mathbf{b}_1-\mathbf{b}_3\equiv\mathbf{q}_\alpha$, since $\mathbf{q}_\alpha$ is defined modulo a reciprocal lattice vector. Similarly, $-\mathbf{q}_\beta\equiv\mathbf{q}_\beta$, and therefore, both amplitudes of (Q_α,Q_β) are real.[32] The critical behavior is determined by the nature of the symmetry invariants of the Landau-Wilson Hamiltonian. Direct inspection shows that $Q_\alpha\rightarrow\pm Q_\alpha$ or $Q_\beta\rightarrow\pm Q_\beta$ for all of the tetragonal symmetry operations. Therefore, the lowest-order symmetry invariant combinations of (Q_α,Q_β) can be chosen as $(Q_\alpha^2+Q_\beta^2)$, $(Q_\alpha^2+Q_\beta^2)^2$, and $(Q_\alpha^4+Q_\beta^4)$, which is identical to the well known $n=2$ XY model with cubic anisotropy.[33] For three spatial dimensions ($d=3$), the stable (isotropic) fixed point for this model gives $2\beta\approx0.70$. However, the asymptotic critical region may be small due to the nearby cubic fixed point. It is therefore likely that our measurements were largely outside the true critical region and we do not regard the disagreement between measured and theoretical values of β as significant.

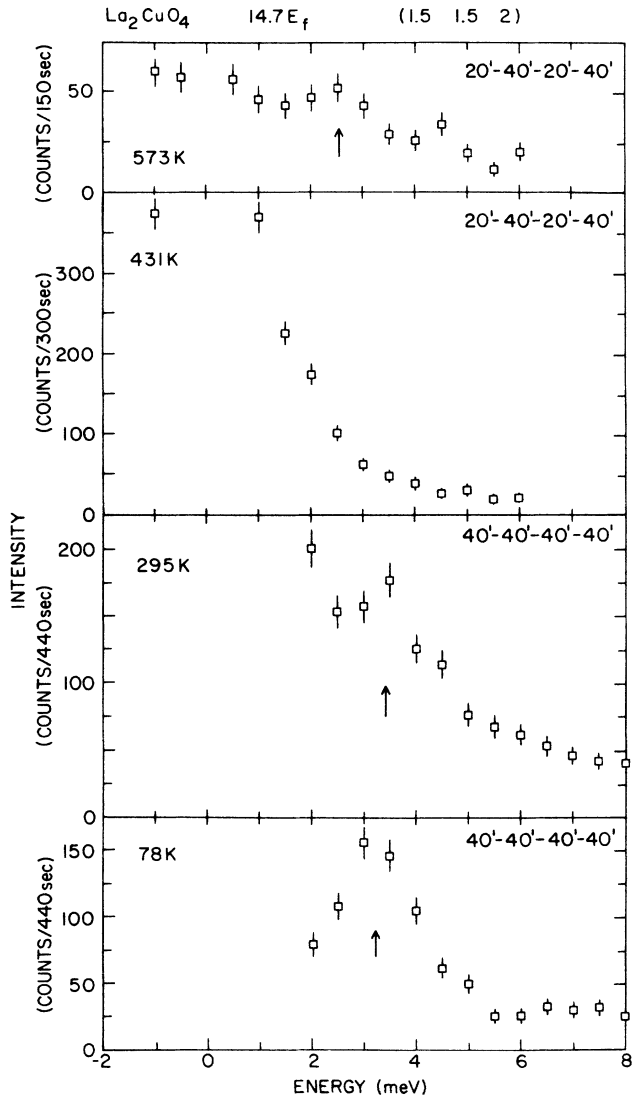

FIG. 2. Temperature dependence of the soft phonon (arrows) near 3 meV (sample MIT-2, $T_0=423$ K) at the superlattice peak position ($\frac{3}{2}$ $\frac{3}{2}$ 2). For similar measurements away from the Bragg position, see Ref. 27. At low temperatures, the soft phonon is very well defined.

IV. PHONONS

A region of reciprocal space suitable for the measurement of the soft TO phonon associated with the structural phase transition was identified near the superlattice peak (1.5 1.5 2). Figure 2 shows some typical scans at the superlattice peak position itself. The soft phonon located near 3 meV disappears with decreasing T at T_0 and strong elastic scattering evolves. Lowering the temperature further leads to the reappearance of a phonon which remains

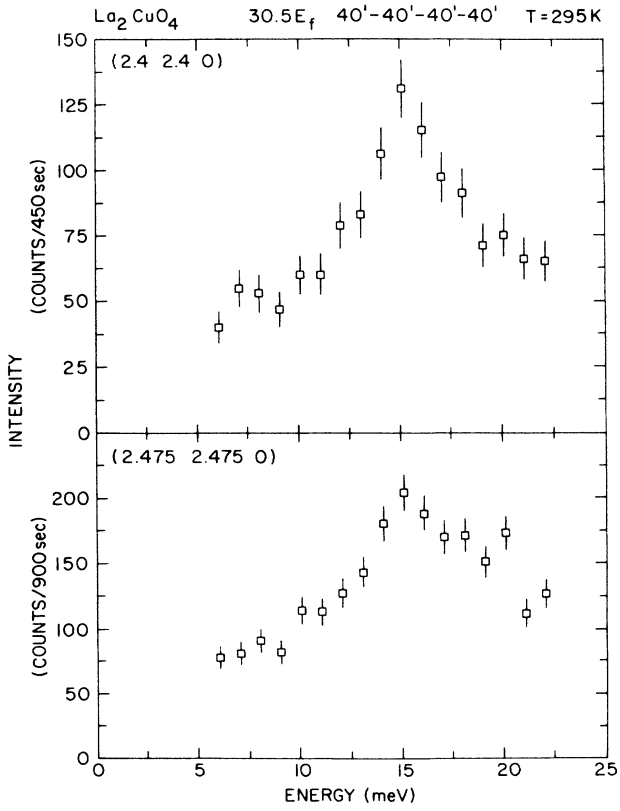

FIG. 3. Typical longitudinal phonon groups near the zone boundary. The phonons exhibit conventional behavior and are well defined (sample MIT-2). In particular, no softening is observed near the zone boundary (2.5 2.5 0).

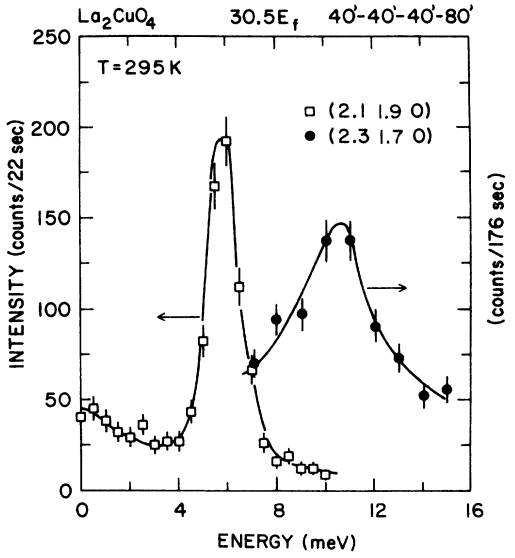

FIG. 4. Spectra of transverse TA_2 phonons measured along [110]. The polarization vector is along [1$\bar{1}$0], i.e., the scattering plane is (hh0) (sample MIT-1).

soft but sharpens significantly. We confirmed by means of additional measurements in other Brillouin zones that this mode has Σ_4 symmetry (in Weber's notation).

Although we expect that the $n=2$ degeneracy is lifted below T_c, we did not observe the expected splitting of the modes, either because the energy resolution of the spectrometer was too coarse or one of the modes renormalizes only weakly and remains buried under the superlattice peak. Further neutron scattering studies are necessary to elucidate this point further.

After identifying the lattice dynamics, which leads to the tetragonal-orthorhombic phase transition, we performed a detailed study of the low-lying phonon branches in order to find evidence for the predicted breathing-mode instability[4] of the LA mode near the zone boundary. The LA phonons were measured in crystals MIT-1 and MIT-2 using very fine steps in momentum in order to find the instability (see Fig. 3 for some representative scans). The phonons remain sharp and the dispersion has a conventional form, i.e., the LA phonon energy increases monotonically with increasing q. This result is in contrast to an observation in isostructural La_2NiO_4 where the phonon energy decreases near the zone boundary. Moreover,

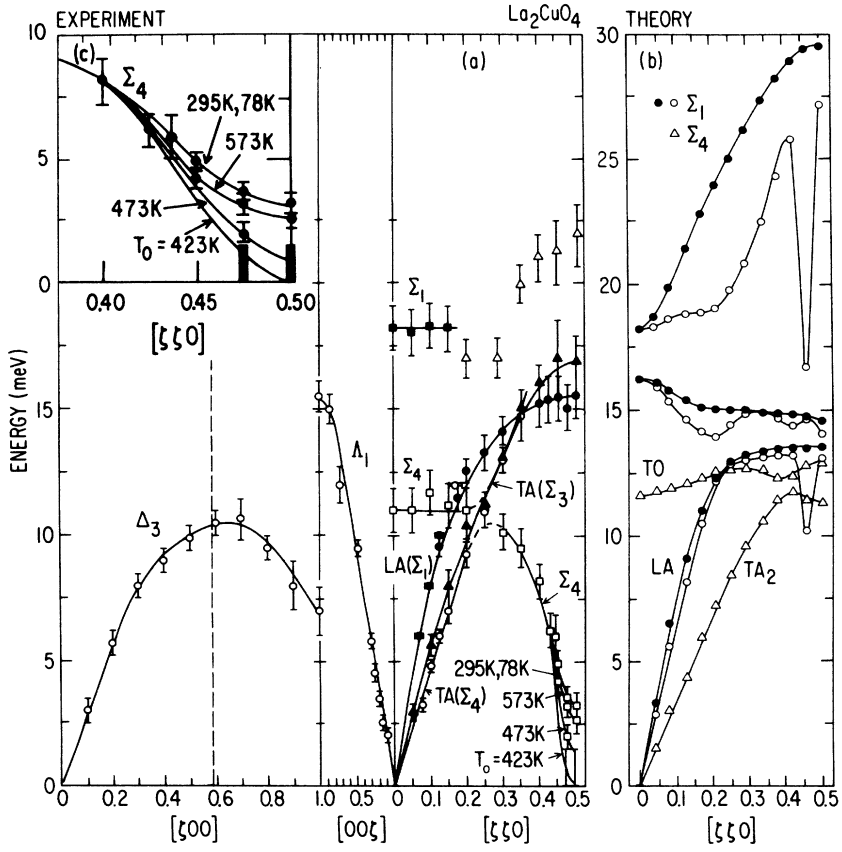

FIG. 5. (a) Summary of the low-lying phonon branches in $La_{2-x}Sr_xCuO_4$ (samples MIT-1 and MIT-2). The lines are guides to the eye. The modes have been labeled according to Ref. 4. The dispersion curves are only weakly temperature dependent, with the exception of the TO phonon near the X point [see inset (c)]. (b) Calculated dispersion curves. Filled symbols show the nonrenormalized energies (bar phonons) and the open circles indicate the phonons with Σ_1 symmetry, which are renormalized by interactions with the conduction electrons. The phonons with Σ_4 symmetry do not renormalize [after Weber (Ref. 4)].

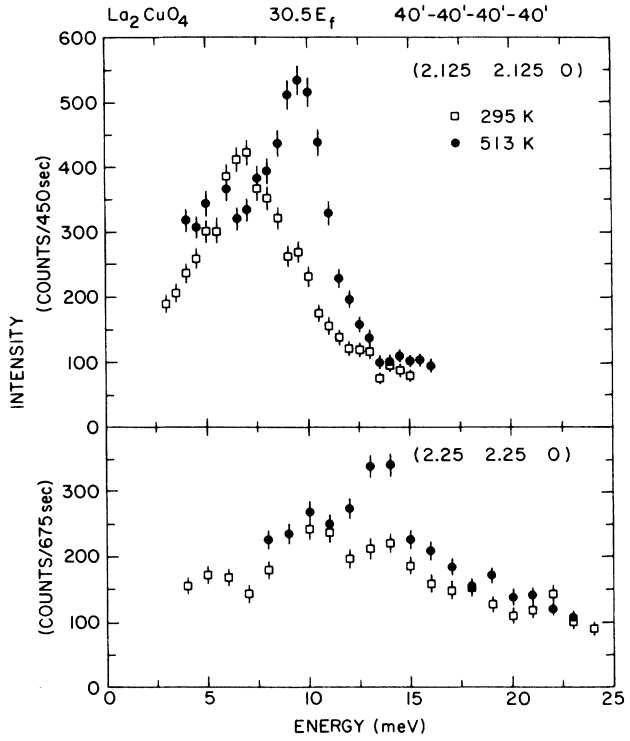

FIG. 6. Longitudinal phonon measurements near (220) for two different temperatures. At small q, the longitudinal phonon intensity decreases roughly like the thermal population factor. At room temperature, a peak evolves near 7 meV (sample MIT-2) at (2.125 2.125 0).

there is no anomalous T dependence of these phonons near T_0 within the accuracy of the measurements. Therefore, our crystals exhibit no breathing-mode instability.

In addition, we spent some time mapping out other low-lying phonon branches. Two typical spectra of in-plane modes (Σ_3 symmetry) are shown in Fig. 4. In Fig. 5, we show a summary of dispersion curves that we have measured in our samples $La_{2-x}Sr_xCuO_4$. The lines through the data points are guides to the eye. The soft mode is identified as a Σ_4 mode and has the same symmetry as the out-of-plane TA_2 mode. Since they are of the same symmetry, they repel each other and exhibit anticrossing behavior.

Figure 6 shows part of an interesting series of LA phonon measurements along the [110] direction at relative small $\mathbf{q}$. Above T_0 we clearly observe sharp peaks which are readily identified as LA phonons. Their intensity decreases with decreasing temperature roughly like the thermal population factor, as expected. At the same time, however, a new peak evolves at smaller energy with an energy of the order of the TA_1 or TA_2 phonon. Such peaks are common in longitudinal scans at small $\mathbf{q}$, when the vertical q resolution of the spectrometer is coarse. This is not the case for the present setup (half width at half maximum, $W_{\mathrm{HWHM}} \simeq 0.08$ Å^{-1}). In addition, the intensity of the transverse phonon would decrease with decreasing temperature in contrast to our observation. Therefore, this peak is not due to a resolution effect. It is most likely that it is caused by a temperature-dependent coupling to an optic mode. The slope of the dispersion yields $v_{\mathrm{LA}} = 5400$ m/s above T_0 and 4000 m/s at room temperature, respectively. The apparent anomalous decrease of v_{LA} is therefore significantly larger than observed in ultrasonic measurements where v_{LA} decreases from 5000 m/s at room temperature to 4640 m/s at 4 K.[34,35]

V. CRITICAL SCATTERING

Figure 7 shows in detail how the critical scattering evolves near T_0 (=351 K) in crystal MIT-1. A momentum- and temperature-independent background of 0.9 counts/s has already been subtracted. The Bragg intensity decreases rapidly on approaching T_0 from below. Above T_0, we observe always a weak, but well defined, resolution-limit central component, superimposed on a

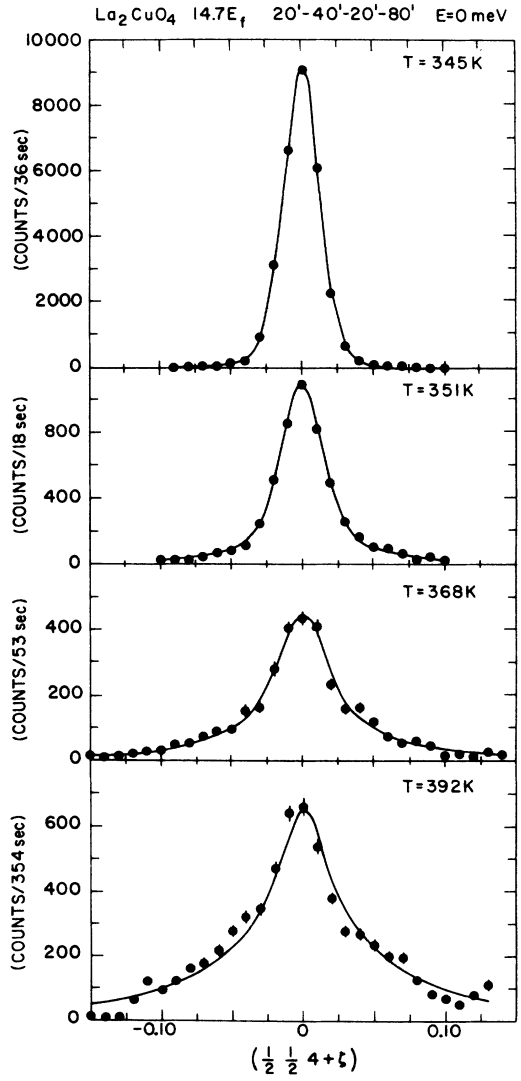

FIG. 7. Typical critical scattering data as measured near the $(\frac{1}{2}\frac{1}{2}4)$ superlattice peak ($T_0 = 351$ K). The solid lines are a parametrization of the data built up by the sum of a (resolution limited) Gaussian and a Lorentzian function (sample MIT-1).

broad diffusive peak. One might argue that the central component is due to a smearing out of the phase transition because of concentration fluctuations in the sample. However, similar investigations on sample MIT-2 show (Fig. 1) that below T_0, the neutron intensity of the superlattice peak scales with the square of the order parameter, or in other words, scales with the strain $a-b$ as measured with x rays. The latter probe is, however, only sensitive to an outer layer of $\simeq 6$ μm of the crystal. Therefore, our samples are quite homogeneous on scales longer than a few microns and it is likely that we indeed observe a "central peak" similar to those observed near the structural phase transitions in the perovskites $SrTiO_3$,[36] $LaAlO_3$,[37] and others,[38] or the famous high-T_c $A15$ superconductor, Nb_3Sn.[39,40]

In order to put our data on a more quantitative basis, we have fitted the critical scattering data to the sum of a Gaussian and a Lorentzian function, namely

$$S(\mathbf{Q}) = I_G \exp\left[-\frac{(\mathbf{Q}-\tau)^2}{2\sigma^2}\right] + I_L \frac{\kappa^2}{(\mathbf{Q}-\tau)^2+\kappa^2}, \quad (1)$$

where τ is a reciprocal-lattice vector. Below T_0, the scattering data were represented well by the Gaussian alone and the half width at half maximum $\Delta q = \sqrt{2\ln 2}\,\sigma$ turned out to have the resolution-limited value $\Delta q = 0.015$ Å^{-1}. In a second step, we fitted all the data to Eq. (1) and found that Δq was independent of temperature. Therefore, we kept σ fixed at its resolution-limited value and extracted from the final fits the amplitudes I_G, I_L, and a correlation length κ. The T dependence of these parameters is shown in Fig. 8. The κ values have been corrected for finite q resolution.

The intensity parameters decrease rapidly with increasing T while κ increases. The solid lines through the data points are an empirical parametrization of the data assuming a power law $[(T_0-T)/T_0]^y$, where $y=\nu$, $-\gamma$, and $-p$ control the temperature dependence of κ, I_L, and I_G, respectively. The critical temperature was fixed at $T_0=351$ K, the value obtained from the T dependence of the $(\frac{1}{2}\ \frac{1}{2}\ 2)$ superlattice peak. We obtain $\nu=0.53\pm0.06$, $p=1.04\pm0.13$, and $\gamma=1.23\pm0.05$ (see Table II). These numbers are related to each other in a reasonable way: $2\beta\sim\nu\sim\frac{1}{2}\gamma$. It is important to point out that I_L and κ are at most qualitatively correct, since the energy window of the spectrometer was only 0.75 meV. Therefore, the energy integration during the course of the experiment is quite likely not complete and the values of the fitted exponents are therefore not likely to be accurate. The exponent p is not affected by the above-mentioned uncertainties because the energy width of the central peak was resolution limited.

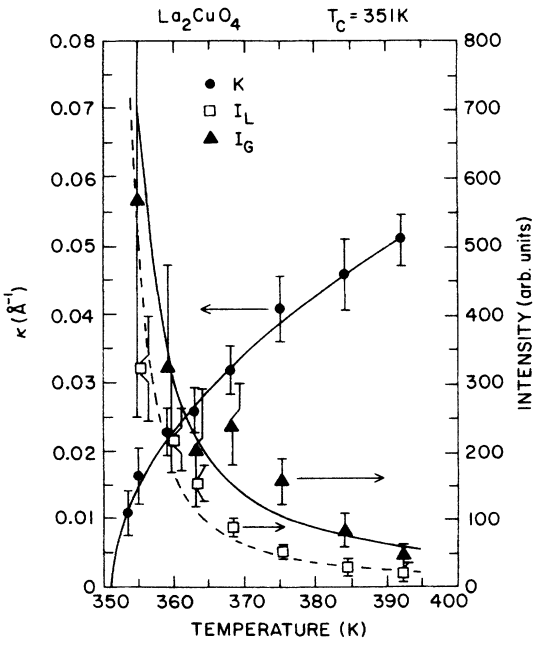

FIG. 8. Temperature dependence of the fit parameters of the data in Fig. 7. The solid lines were used to parametrize κ and I_G. The broken line is for I_L. For details, see text and Table II.

A general understanding of the central-peak phenomena is still incomplete. It is clear that stress from either static[41] or quasistatic[42] defects that coupled to the soft mode in a proper way (linear in the soft-mode order parameter) can cause a central peak. The soft-mode strain field that builds up under these conditions is proportional to the soft-mode susceptibility [i.e., $(T-T_0)^{-\gamma}$]. Since the central peak intensity is proportional to the square of the displacements one expects $p=2\gamma$. However, strongly coupled and slowly relaxing terms in the phonon self-energy (intrinsic or of defect origin) can also give rise to central-peak intensities proportional to the soft-mode susceptibility ($p=\gamma$),[41,42] more nearly in agreement with our observation, for T close to T_0. This is a complex subject requiring further study, but it will not be pursued further here.

VI. DISCUSSION

First we compare our data with other experiments. The dispersion curves from $La_{2-x}Sr_xCuO_4$ compare qualitatively well with those obtained by Pintschovius *et al.*[17] in isostructural La_2NiO_4. There are, however, some differences which are important with regard to possible mechanisms for superconductivity. There is no softening of the LA mode near the zone boundary in La_2CuO_4, and conversely, the TO phonon which is responsible for the tetragonal-to-orthorhombic phase transition is significantly harder in La_2NiO_4 ($\simeq 7$ meV) than in $La_{2-x}Sr_xCuO_4$. We conclude that although the lattice dynamics of La_2NiO_4 is interesting in itself, it is not a good reference system for La_2CuO_4 and possible coincidences with band calculations of La_2CuO_4 (Ref. 4) cannot be taken too seriously.

Despite the fact that our present measurements cover only the low-energy part of the phonon dispersion, it is instructive to compare the results with recent phonon density-of-states measurements by Renker *et al.*[16] From Fig. 5, we infer that the density of states is high for extrema of the phonon dispersion curves, which occur mostly around 10.5 and 17 meV. Indeed, peaks are observed near these positions in superconducting and nonsuperconducting samples of $La_{2-x}Sr_xCuO_4$ (see also Ref. 43). These vibrations involve mostly La motions. Our measurements

offer also an explanation for the lower density of states around 4 meV at $T=300$ K in the superconducting powder sample ($x=0.15$) when compared with the nonsuperconducting samples,[16] namely, the soft TO phonon has stiffened and is better defined in the latter sample which is well within the orthorhombic phase whereas the former sample is still tetragonal.[31] The lower density of states at low energies just reflects the fact that the soft phonon is more damped and its spectral weight is more distributed in energy.

Because $La_{2-x}Sr_xCuO_4$ is opaque and the growth of single crystals is difficult, there is not much light-scattering data available. In Table III we compare some Raman data[18-20,44] and some theoretical results with neutron scattering data at $q=0$. The comparison shows that the mode assignment in the Raman experiments is not unique and that the reported frequencies deviate from experiment to experiment. Since the measurements by Čopič *et al.*[20] were done with polarization analysis, their mode assignment is most convincing and the reported frequencies indeed agree well with Weber's[4] calculations. Obviously, the assignment of the two lowest-lying modes in Ref. 19 should be reversed in order to be in qualitative agreement with the other work. It is remarkable how well the Raman frequencies from isostructural Sr_2TiO_4 (Ref. 44) agree with the results from La_2CuO_4 when the frequencies are scaled properly, indicating that the modes at $q=0$ behave in a conventional fashion.

Next, we compare our data with recent theoretical calculations. Table III shows that the phonon data at $q=0$ are in reasonable agreement with the phonon frequencies derived from band calculations.[4] This is not surprising, since a Born-von Kármán force-constant model based on neutron data from $Ba(Pb,Bi)O_3$ (Ref. 45) was used for the derivation of the bare phonon part in the band calculation. At finite q, however, we observe serious discrepancies of the model with experiment. First, we do not observe any evidence of the predicted softening of the oxygen breathing mode[4] [Fig. 5(b)], which lowers the energies of the Σ_1 branches significantly near the zone boundary. Second, the modes are well defined and there is no broadening which would indicate a strong electron-phonon coupling. Further, the theory does not indicate any softening of the TO phonon (Σ_4) that drives the tetragonal-orthorhombic phase transition. Since the predicted soft breathing mode is the result of strong screening contributions from electrons near the Fermi surface, it is possible that the smearing of the Fermi surface, which is implied by the observed hoppinglike conductivity,[29] also serves to remove or greatly reduce the softness of the breathing mode. This possibility could be most directly tested if efforts to produce modifications of the La_2CuO_4 system with conventional metallic transport properties prove successful.

Comparing the experimental data with the prediction of the PIB model from Ref. 28, which attempts to calculate the bare force constants in a less empirical manner, the quantitative agreement with the $q=0$ data is not good (Table III). This is expected, given the nonempirical nature of the model. Actually, it is noteworthy that the calculated energies at $q=0$ agree reasonably well with experiment when they are scaled by $\frac{1}{2}$. The energies are too large because of the neglect of screening and nonspherical charge deformations.[28] However, the model predicts correctly the softening of the TO phonon at the X point which initiates the tetragonal-orthorhombic phase transition. Moreover the oxygen breathing mode is stable, as observed in our experiment.

Table IV shows a detailed comparison of (powder) superlattice peak intensities calculated by using displacements derived from minimum energy structures in the PIB model with those calculated from the soft-phonon eigenvector of the PIB model and with the experimental powder diffraction intensities.[14,46] TF uses the Thomas-Fermi kinetic energy, whereas KS uses the Kohn-Sham kinetic energy for the self-energy of the ions and the Thomas-Fermi kinetic energy for the overlap contribution (see Ref. 28). If we use as a criterion for the best model the sum of squares of the deviations, weighted by the intensity of the experimental intensities, then the TF model is favored, although some predicted intensities are off by orders of magnitude for both models. On the other hand, the experimental volume is closer to the equilibrium volume of the KS model than of the TF model.[28] We consider the agreement between experiment and the frozen soft-phonon calculation as most favorable, because of the

TABLE III. Comparison of Raman and neutron scattering data (energies are given in meV)[a] with a band model and a potential induced breathing (PIB) model.

This work	Ref. 18	Ref. 19	Ref. 20	Ref. 44[b]	Ref. 4	Ref. 28[c]
		$La_{2-x}Sr_xCuO_4$		Sr_2TiO_4	E bands	PIB
11.0 ± 1 (Σ_4)		12.4 (Σ_1)		12.2	11.7 (Σ_4)	−6.7 (Σ_4)
18.4 ± 1 (Σ_1)	19.0	22.3 (Σ_4)	17.1 (Σ_1)	20.1	16.2 (Σ_1)	37.6 (Σ_1)
			26.1 (Σ_4)	28.1	29.8 (Σ_4)	41.7 (Σ_4)
	82.3		33.5			
	96.0	47.1 (Σ_1)	51.1 (Σ_1)	56.9	55.8 (Σ_1)	83.8 (Σ_1)

[a]It may be useful to note the following equivalences of the symbols for the irreducible representations of the Raman active modes in tetragonal La_2CuO_4: $A_{1g}\equiv\Gamma_{1+}$ and $E_g\equiv\Gamma_{5+}$. Along the Σ line: $\Gamma_{1+}\rightarrow\Sigma_1$ and $\Gamma_{5+}\rightarrow\Sigma_2+\Sigma_4$. Conversion factors for energies: 1 meV = 8.07 cm^{-1} = 0.2418 THz.

[b]The frequencies reported in Ref. 44 for Sr_2TiO_4 have been multiplied by $\sqrt{m_{Sr}/m_{La}}=0.79$.

[c]The negative frequency corresponds to an unstable mode.

TABLE IV. Comparison of calculated peak intensities (Ref. 28) with observation (Refs. 14 and 46).

Cmca	*I4/mmm*	KS	TF	Soft phonon	Experiment
021	0.5 0.5 2	11.2	0.2	37.2	16.4
041	0.5 0.5 4	165.9	131.3	51.8	88.3
221	0.5 1.5 2	114.7	98.2	156.8	65.1
061	0.5 0.5 6	0.6	32.6	37.0	10.3[a]
241	0.5 1.5 4	6.8	6.1	0.5	1.6
023	1.5 1.5 2	3.8	61.3	98.3	119.8
261	0.5 1.5 6	92.5	84.3	14.9	55.7
043	1.5 1.5 4	30.8	0.5	10.0	51.5
081	0.5 0.5 8	0.0	11.9	19.9	17.7
Sum of intensities		426.3	426.3	426.5	426.4
σ^2		296.1	210.3	308.3[b]	

[a]The $(\frac{1}{2}\ \frac{1}{2}\ 6)$ reflection is difficult to measure in powder scans because of the proximity of an Al line.
[b]Variance: $\sigma^2=\sum_{hkl}(I^{hkl}_{\text{expt}}-I^{hkl}_{\text{calc}})^2/I^{hkl}_{\text{expt}}$.

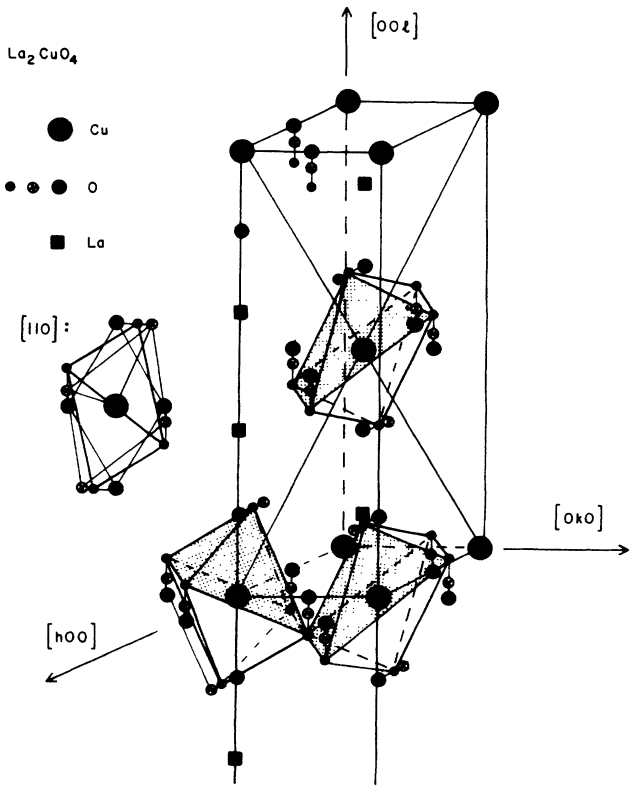

FIG. 9. Visual representation of the tilting of the oxygen octahedra around the Cu atoms. The solid circles of medium size show the position of the oxygen atoms in the tetragonal phase. The small solid circles represent the frozen tilting mode as predicted by the ionic PIB model. The open circles with the cross (⊗) reproduce the tilting of the octahedra as observed in experiment (Refs. 13 and 14). The projection in the [110] direction shows that the predicted tilting goes along with a very serious distortion of the octahedra, in contrast to the almost rigid tilting in experiment.

agreement in the overall pattern of strong and weak reflections and because the intensities are only off by factors of 5 or less. The soft-phonon eigenvector predicts that the oxygen octahedra become very distorted in the orthorhombic phase (Fig. 9) whereas experiment indicates that the octahedra tilt almost rigidly around the Cu atoms. Inclusion of screening and nonspherical charge deformations in the ionic model may remove some of the discrepancies.

What effect, if any, do the soft X-point phonons have upon T_c? Roughly speaking, conventional weak-coupling Bardeen-Cooper-Schrieffer theory predicts $T_c \propto \langle\omega\rangle \times \exp(-\langle\omega^2\rangle/\rho I)$, where $\langle\omega\rangle$ and $\langle\omega^2\rangle$ are the first and second moments of the phonon energies, ρ the density of states at the Fermi surface, and I the electron-phonon coupling. The presence of frequency averages in both the exponential and the preexponential terms suggests the notion of an optimized phonon system, which must be stiff enough to provide a large energy scale but soft enough to be easily polarizable by the electrons.[47] Thus, while it seems likely that under suitable conditions soft phonons can enhance superconductivity, it is less clear that selective softening of a small fraction of phonons in an isolated region of reciprocal space, such as we find in La_2CuO_4, can provide enough leverage to produce a significant effect. Then there is the question how effectively the soft mode couples to the electrons. While rotational motions seem at first sight less well suited in this regard than breathing modes, Cohen[28(b)] suggests that the significantly increased electron density of states near the Fermi energy in the orthorhombic phase yields a moderate electron-phonon coupling. Moreover, an isotope effect[48] has been observed in $La_{2-x}Sr_xCuO_4$, suggesting that the lattice dynamics is not totally irrelevant for the occurrence of a superconducting state, although our present understanding of isotopic substitution on superconducting transition temperatures in general is inadequate (e.g., the Pd-H system[49]). Further circumstantial support is supplied by the observation that T_0 decreases with increasing

doping driving the system closer to the structural stability at temperatures near T_c. This situation is similar to that in the $A15$ superconductor Nb_3Sn where the structural phase transition occurs at $T_0 \simeq 45$ K, not far above $T_c = 18$ K.[39]

According to Mattis and Mattis[50] the in-plane bond asymmetry in the orthorhombic phase and the quasi-two-dimensional nature of the Fermi surface are essential ingredients for high T_c as long as some kind of attractive two-body potential exists (for example, phonons or spin fluctuations). Soft phonons are often associated with such symmetry-lowering phase transitions. The interplay between the structural phase transition and the magnetism has recently been discussed by Thio *et al.*[51]

Finally, we would like to summarize the most important conclusions. The tetragonal-orthorhombic phase transition in $La_{2-x}Sr_xCuO_4$ is caused by a classical soft-phonon transition at the X point similar to that observed in many perovskites.[38] The most important structural difference between the perovskites [$T_c \simeq 0.3$ K for $SrTiO_{3-\delta}$ (Ref. 52)] and $La_{2-x}Sr_xCuO_4$ is probably the two-dimensional nature of the latter, which may have important implications on the electron-phonon coupling. The measured energies agree well with ultrasonic and some Raman measurements where the data overlap. A PIB model accounts qualitatively for the observed transition which predicts correctly that it is not induced by a condensed oxygen breathing mode. With the exception of the X-point anomaly, the phonon spectra observed to date exhibit a rather conventional behavior and no further striking anomalous features are observed which appear to be related to high-T_c superconductivity. This statement fits well into the more general observation that superconducting properties show up most clearly in transport measurements and not in the lattice dynamics itself. While our results neither confirm nor rule out the general importance of phonon-mediated interactions for high T_c, they give no support to the proposed breathing-mode mechanism. Our measurements provide, however, data against which future theories must be tested.

ACKNOWLEDGMENTS

We would like to thank P. B. Allen, R. E. Cohen, D. E. Cox, T. Freltoft, S. Mitsuda, S. M. Shapiro, and W. Weber for very fruitful discussions. This work is supported by the Division of Materials Sciences, U.S. Department of Energy under Contract No. DE-AC02-76CH00016 and by National Science Foundation Grants No. DMR 85-01856 and No. DMR 84-18718.

*Permanent address: Paul Scherrer Institute (PSI), Labor für Neutronenstreuung, Eidgenössische Technische Hochschule, 5303 Würenlingen, Switzerland.

[1]J. G. Bednorz and K. A. Müller, Z. Phys. B **64**, 189 (1986).

[2]C. W. Chu, P. H. Hor, R. L. Meng, L. Gao, Z. J. Huang, and Y. Q. Wang, Phys. Rev. Lett. **58**, 405 (1987).

[3]L. F. Mattheiss, Phys. Rev. Lett. **58**, 1028 (1987).

[4]W. Weber, Phys. Rev. Lett. **58**, 1371 (1987). We thank W. Weber for sending us the details of his calculations and for many helpful discussions.

[5]J. Yu, A. J. Freeman, and J.-H. Xu, Phys. Rev. Lett. **58**, 1035 (1987).

[6]C. L. Fu and A. J. Freeman, Phys. Rev. B **35**, 8861 (1987).

[7]A. J. Freeman, J. Yu, and C. L. Fu, Phys. Rev. B **36**, 7111 (1987).

[8]P. W. Anderson, G. Baskaran, Z. Zou, and T. Hsu, Phys. Rev. Lett. **58**, 2790 (1987).

[9]R. A. Zacher, Phys. Rev. B **36**, 7115 (1987).

[10]V. J. Emery, Phys. Rev. Lett. **58**, 2794 (1987).

[11]J. E. Hirsch, Phys. Rev. Lett. **59**, 228 (1987).

[12]Any omission of important experimental and theoretical work was not anticipated.

[13]Von B. Grande, Hk. Müller-Buschbaum, and M. Schweizer, Z. Anorg. Allg. Chem. **428**, 120 (1977).

[14]J. D. Jorgensen, H.-B. Schüttler, D. G. Hinks, D. W. Capone II, K. Zhang, M. B. Brodsky, and D. J. Scalapino, Phys. Rev. Lett. **58**, 1024 (1987).

[15]P. M. Grant, S. S. P. Parkin, V. Y. Lee, E. M. Engler, M. L. Ramirez, J. E. Vazquez, G. Lim, R. D. Jacowitz, and R. L. Greene, Phys. Rev. Lett. **58**, 2482 (1987).

[16]B. Renker, F. Gompf, E. Gering, N. Nücker, D. Ewert, W. Reichardt, and H. Rietschel, Z. Phys. B **67**, 15 (1987).

[17]L. Pintschovius, J.-M. Bassat, P. Odier, F. Gervais, B. Hennion, and W. Reichardt, Europhys. Lett. **5**, 247 (1988).

[18]S. Sugai, M. Sato, and S. Hosoya, Jpn. J. Appl. Phys. **26**, L495 (1987).

[19]S. Blumenroeder, E. Zirngiebl, J. D. Thompson, P. Killough, J. L. Smith, and Z. Fisk, Phys. Rev. B **35**, 8840 (1987).

[20]M. Čopič D. Mihailović, M. Zgonik, M. Prester, K. Biljaković, B. Orel, and N. Brničević, Solid State Commun. **64**, 297 (1987).

[21]T. A. Faltens, W. K. Ham, S. W. Keller, K. J. Leary, J. N. Michaels, A. M. Stacy, H.-C. zur Loye, D. E. Morris, T. W. Barbee III, L. C. Bourne, M. L. Cohen, S. Hoen, and A. Zettl, Phys. Rev. Lett. **59**, 915 (1987).

[22]B. Batlogg, G. Kourouklis, W. Weber, R. J. Cava, A. Jayaraman, A. E. White, K. T. Short, L. W. Rupp, and E. A. Rietman, Phys. Rev. Lett. **59**, 912 (1987).

[23]K. J. Leary, H.-C. zur Loye, S. W. Keller, T. A. Faltens, W. K. Ham, J. N. Michaels, and A. M. Stacey, Phys. Rev. Lett. **59**, 1236 (1987).

[24]D. Vaknin, S. K. Sinha, D. E. Moncton, D. C. Johnston, J. M. Newsam, C. R. Safinya, and H. E. King, Jr., Phys. Rev. Lett. **58**, 2802 (1987).

[25]J. M. Tranquada, D. E. Cox, W. Kunnmann, H. Moudden, G. Shirane, M. Suenaga, P. Zolliker, D. Vaknin, S. K. Sinha, M. S. Alvarez, A. J. Jacobsen, and D. C. Johnston, Phys. Rev. Lett. **60**, 156 (1988).

[26]G. Shirane, Y. Endoh, R. J. Birgeneau, M. A. Kastner, Y. Hidaka, M. Oda, M. Suzuki, and T. Murakami, Phys. Rev. Lett. **59**, 1613 (1987).

[27]R. J. Birgeneau, C. Y. Chen, D. R. Gabbe, H. P. Jenssen, M. A. Kastner, C. J. Peters, P. J. Picone, T. Thio, T. R. Thurston, H. L. Tuller, J. D. Axe, P. Böni, and G. Shirane, Phys. Rev. Lett. **59**, 1329 (1987).

[28](a) R. E. Cohen, W. E. Pickett, H. Krakauer, and L. L. Boyer, Physica B (to be published); Phys. Rev. Lett. **60**, 817 (1988); (b) R. E. Cohen (private communication).

[29]M. A. Kastner, R. J. Birgeneau, C. Y. Chen, Y. M. Chiang, D. R. Gabbe, H. P. Jenssen, T. Junk, C. J. Peters, P. J. Pi-

cone, Tineke Thio, T. R. Thurston, and H. L. Tuller, Phys. Rev. B **37**, 111 (1988).

[30]Y. Endoh, K. Yamada, R. J. Birgeneau, D. R. Gabbe, H. P. Jenssen, M. A. Kastner, C. J. Peters, P. J. Picone, T. R. Thurston, J. M. Tranquada, G. Shirane, Y. Hidaka, M. Oda, Y. Enomoto, M. Suzuki, and T. Murakami, Phys. Rev. B **37**, 7443 (1988); Y. Hidaka, Y. Enomoto, M. Suzuki, M. Oda, and T. Murakami, Jpn. J. Appl. Phys. **26**, L377 (1987).

[31]R. M. Fleming, B. Batlogg, R. J. Cava, and E. A. Rietman, Phys. Rev. B **35**, 7191 (1987).

[32]In general $Q_\alpha \equiv Q(\mathbf{q}_\alpha) = Q(-\mathbf{q}_\alpha)^*$, so that if $\mathbf{q}_\alpha = -\mathbf{q}_\alpha$ then $Q(\mathbf{q}_\alpha) = Q(\mathbf{q}_\alpha)^*$, and similarly for $Q(\mathbf{q}_\beta)$.

[33]A. Aharony, Phys. Rev. B **8**, 4270 (1973).

[34]Y. Horie, T. Fukami, and S. Mase, Solid State Commun. **63**, 653 (1987).

[35]D. J. Bishop, P. L. Gammel, A. P. Ramirez, R. J. Cava, B. Batlogg, and E. A. Rietman, Phys. Rev. B **35**, 8788 (1987).

[36]S. M. Shapiro, J. D. Axe, G. Shirane, and T. Riste, Phys. Rev. B **6**, 4332 (1972), and references therein.

[37]J. K. Kjems, G. Shirane, K. A. Müller, and H. J. Scheel, Phys. Rev. B **8**, 1119 (1973).

[38]For a review, see G. Shirane, Rev. Mod. Phys. **46**, 437 (1974).

[39]J. D. Axe and G. Shirane, Phys. Rev. B **8**, 1965 (1973).

[40]G. Shirane and J. D. Axe, Phys. Rev. Lett. **27**, 1803 (1971).

[41]For a detailed discussion, see Ref. 39.

[42]B. I. Halperin and C. M. Varma, Phys. Rev. B **14**, 4030 (1976).

[43]A. P. Ramirez, B. Batlogg, G. Aeppli, R. J. Cava, E. Rietman, A. Goldman, and G. Shirane, Phys. Rev. B **35**, 8833 (1987).

[44]G. Burns, F. H. Dacol, and M. W. Shafer, Solid State Commun. **62**, 687 (1987).

[45]W. Reichardt, B. Batlogg, and J. Remeika, Physica B **135**, 501 (1985), and unpublished data.

[46]J. D. Jorgensen (private communication).

[47]P. B. Allen, in *Dynamical Properties of Solids,* edited by G. K. Horton and A. A. Maradudin (North-Holland, Amsterdam, 1980), Vol. 3, p. 95.

[48]Even a vanishing isotope effect does not rule out an electron-phonon coupling. See J. C. Swihart, Phys. Rev. **116**, 45 (1959).

[49]B. Stritzker and W. Buckel, Z. Phys. **257**, 1 (1972).

[50]D. C. Mattis and M. P. Mattis, Phys. Rev. Lett. **59**, 2780 (1987).

[51]Tineke Thio, T. R. Thurston, N. W. Preyer, P. J. Picone, M. A. Kastner, H. P. Jenssen, D. R. Gabbe, C. Y. Chen, R. J. Birgeneau, and A. Aharony, Phys. Rev. B (to be published).

[52]C. S. Koonce, M. L. Cohen, J. F. Schooley, W. R. Hosler, and E. R. Pfeiffer, Phys. Rev. **163**, 380 (1967).

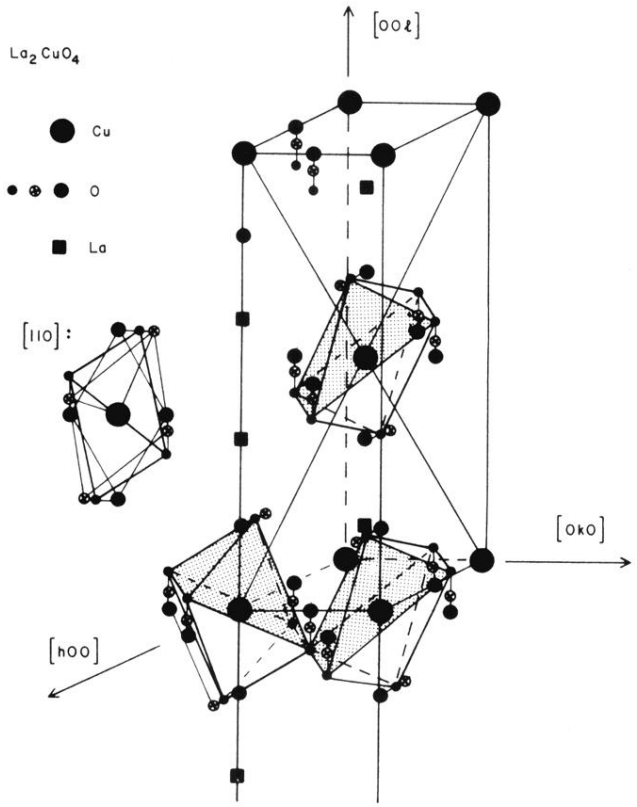

FIG. 9. Visual representation of the tilting of the oxygen octahedra around the Cu atoms. The solid circles of medium size show the position of the oxygen atoms in the tetragonal phase. The small solid circles represent the frozen tilting mode as predicted by the ionic PIB model. The open circles with the cross (⊗) reproduce the tilting of the octahedra as observed in experiment (Refs. 13 and 14). The projection in the [110] direction shows that the predicted tilting goes along with a very serious distortion of the octahedra, in contrast to the almost rigid tilting in experiment.